Model for surface cracking

Horacio Colina, Lucilla de Arcangelis, and Stéphane Roux
Laboratoire de Physique et Mécanique des Milieux Hétérogènes,
Ecole Supérieure de Physique et Chimie Industrielles, 10 rue Vauquelin, 75231 Paris Cedex 05, France
(Received 10 February 1993)

We introduce a network model to study the cracking of the surface of a material subjected to an imposed strain along one boundary, or to a surface shrinkage induced by drying or cooling. The model we study is an electrical analog of the mechanical problem, and consists in a network of fuses whose breaking thresholds are randomly distributed. The coupling with a substrate, where a uniform electric field is applied, models the hindering to shrinking of the mechanical problem. Some analytical results are derived for the one-dimensional version of this model. In two dimensions, we study numerically a number of mechanical and geometrical properties for two distributions of breaking strengths and make a qualitative comparison with experimental results.

I. INTRODUCTION

The damage and fracture of disordered media has recently attracted[1-3] a lot of attention in particular in connection with the phenomenon of "localization." In some cases, the homogeneous deformation field in a solid is no longer stable but it begins to get spatially confined to a narrow region. This phenomenon has a number of consequences. For instance, the measured stress-strain relation during a mechanical test is no longer representative of a behavior law of the entire material but combines both the effect of the mechanical behavior and that of dishomogeneties of the strain field due to localization.

Heterogeneities have the tendency to delay the occurrence of localization and to affect the small scale stress and strain field in the localized region. Hence, their role is to be understood in order to achieve a better description of the damage process and its range of validity. One of the consequences of the localization is that the macroscopic behavior becomes crucially dependent on the size of the localized region. Therefore, disorder gives rise to unexpected size effects and shape effects that cannot be described without explicitly considering the heterogeneities.

It is therefore extremely important to identify the length scales, which are involved in a fracture process, as well as to characterize the effect of the boundary conditions. In particular, in connection with the latter point, a new mechanical test has been recently proposed[4,5] in order to prevent localization, and thus to reveal the mechanical behavior of a material in a regime where this is difficult to identify. The principle of this test consists in imposing a strain along the border of the sample instead of a stress. For instance a concrete specimen can be glued to two aluminum plates, which are subjected to a traction. The elastic limit of the aluminum plates is much higher than the one of concrete and thus the strain can be considered as homogeneous. The glued interface transmits the strain to the concrete sample. It is obvious under those conditions that a crack in the concrete part will develop along a plane normal to the tensile stress and thus perpendicularly to the aluminum plate. Therefore, the presence of cracks will not prevent the further damage of the sample. However, the stress distribution in the vicinity of a crack is an essential element in the interpretation of this test, and a close analysis of this geometry reveals the occurrence of a length scale, which is characteristic of the interface (glue, roughness of the sample surface, rheology of the tested material, etc.).

The simple numerical model we introduce here aims at investigating the scaling behavior of fracture of disordered media with a loading condition, which is close to the previous testing conditions. Such a model may also give some insights to the problem of fracture induced by

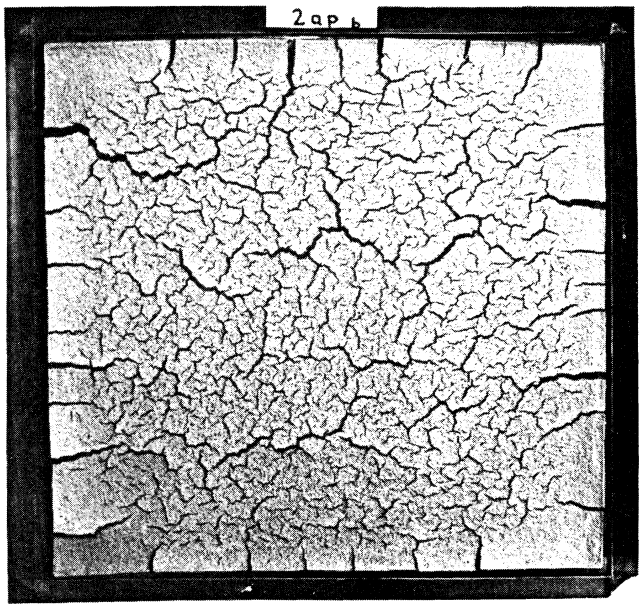

FIG. 1. Fracture pattern obtained on a thin layer of clay (20 cm×20 cm×2 mm). The cracks were created as a result of the shrinking of the clay after drying for about 7 h.

differential shrinking or swelling which occurs for instance in clay or concrete when fresh samples are drying from a surface.[6,7] Figure 1 shows such an example of fracture pattern obtained on a thin layer of clay deposited on a rigid substrate. The geometry of the fracture patterns generated in such conditions are very common, and can be seen on many walls or drying clay. Let us also mention that we will show a few results for a one-dimensional version of the model, which are relevant for the fracture of fiber-reinforced ceramic composites, as recently developed by Curtin[8] and Hild.[9]

II. NETWORK MODEL

In order to model the cracking of a surface, one can consider a two-dimensional heterogeneous network of elements whose breaking characteristics are brittle. Previous work using this description has been published by Meakin.[7] All the elements have the same elastic behavior, i.e., the same elastic constant, but their breaking thresholds are randomly assigned following a given distribution. The external loading is applied to the system via the coupling to a stiff substrate. Namely, each site of the system is connected by an elastic bond to a lower network where a uniform deformation is applied. All the coupling bonds are identical and not susceptible to breaking.

One needs next to specify the nature of the elements of the system. A natural choice is to consider a network of elastic springs; however, this raises some problems in order to identify the cracks in a simple geometrical way. In fact, due to the free rotation of the springs at the nodes, it is possible to obtain a real fracture between two elastic blocks even if the set of broken bonds does not form a connected cluster in the dual lattice.[10] This problem can be avoided by considering a network of elastic beams fixed at the nodes of the lattice.[11] In this case, however, several parameters must be introduced to characterize the elastic and breaking behavior of each element.

We have chosen to simplify the problem by considering an electrical analog. Previous detailed comparisons[12] between mechanical network models and electrical analog have revealed that the scaling properties of those models were quite similar, but the simplicity of the electrical scalar problem leads to a more efficient numerical program and thus larger system sizes and better statistics can be achieved. The system is a $L \times L$ square lattice at 45° of electrical fuses having equal unit conductance and randomly assigned breaking threshold. The substrate is a similar network, where the external potential is applied at the nodes via a uniform electric field. The fuse network is coupled to the substrate by electrical resistors of conductance g_c as shown in Fig. 2. The conductance g_c is a free parameter of the problem and can be compared to the inverse thickness of the layer of drying material as we will discuss below. Periodic boundary conditions are used in both the direction parallel and perpendicular to the applied field for the current and the voltage drop. A discontinuity in the potential must therefore be taken into account along the direction of the field to allow for a nonzero mean current density.

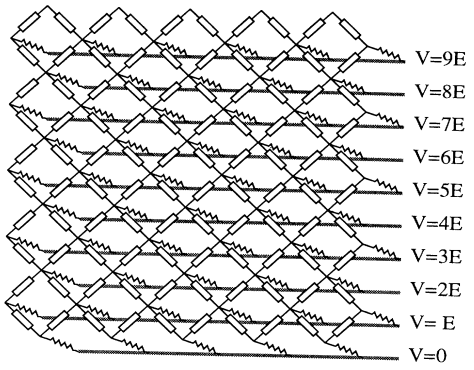

FIG. 2. Our electrical analog model is represented by a two-dimensional lattice of fuses (white elements) coupled by resistors to a set of sites where a uniform electric field E is imposed.

The simulation is performed along the same method as used in earlier work with different systems.[10–14] A potential difference is applied to the substrate and the local currents are calculated using the conjugate gradient algorithm to a precision $\epsilon = 10^{-8}$. For all the fuses the ratio of the flowing current j to the breaking threshold j_c is evaluated and the fuse for which the value of this ratio j/j_c is maximum, is removed (i.e., its conductance is set to zero). The local currents are therefore calculated again in order to determine the fuse to break next. At each step the external potential is adjusted so that only one fuse reaches its threshold value, and thus breaks. The process is continued until a macroscopic crack appears, whose projection on the direction perpendicular to the field is equal to the linear size of the system L.

During the breaking process a number of "mechanical" (or rather their electrical analogs) and geometrical properties are monitored and averaged over several initial configurations of bonds. The results are discussed in the following sections. In order to investigate the influence of the disorder on the behavior of the system, we analyze two different cases: a *strong disorder* situation where the breaking thresholds are drawn from a uniform distribution between zero and one; and a *weak disorder* situation where they are uniformly distributed between one and two. Those two kinds of distribution have been studied extensively in the past for usual loading (a voltage drop imposed across the network), respectively, in Refs. 13 and 14. Moreover, for each disorder case different values of the coupling conductance g_c are analyzed. As we will see later, this parameter is related to a characteristic length ξ of the problem. The range of ξ considered goes from the lattice constant up to the system size.

As a final remark we want to point out that this particular choice of a scalar model, definitely convenient from the numerical point of view, represents a strong simplification of the problem. Moreover, the presence of an electric field introduces a preferential direction for the cracks, which tend to align perpendicularly to the field. In the case of an isotropic shrinking of the surface of a brittle solid, this is evidently not the case. However, in

the case of the mechanical test designed to avoid localization mentioned in the Introduction, the uniaxial extension imposed on the surface introduces a comparable orientational effect.

Therefore one cannot expect to obtain from the model results to compare quantitatively with the experimental data, but it is reasonable to think that the qualitative behavior observed for the model can give useful insights to the physics of the problem, and allows to identify scaling regimes faithfully.

III. COUPLING LENGTH

The value of the conductance g_c coupling the system to the substrate is a fundamental parameter of the model. More precisely, the ratio of g_c to the conductance of the fuses, equal to unity in our model, introduces a characteristic length ξ, that represents the range of influence of a missing fuse. In an experimental situation, like the one mentioned before of a thin layer of clay drying on a substrate, this length combines at the time the effects of the thickness of the layer and the elastic coupling between the clay and the substrate. In the test mentioned in the Introduction as well as for fibers in reinforced composite materials, a similar problem arises from the coupling between two different materials.

This notion of coupling length can be well understood in the framework of a one-dimensional model. The network (Fig. 3) is a one-dimensional chain of fuses coupled by the conductances g_c to the substrate. The external potential at the site n of the substrate is simply $U_n = nE$, where E is the electric field. When all the fuses are present, the current is constant in the chain of fuses and the potential at the node n between two fuses is $V_n = U_n$.

Let us suppose now that the fuse between $n=-1$ and 0 has been broken (Fig. 3) and let us evaluate the potentials V_n at the nodes of the chain. The conservation law of the current at each node $n \geq 1$ can be written as

$$V_{n+1} - V_n = V_n - V_{n-1} + (g_c/2)(V_n - U_n) \ . \tag{1}$$

Since far from the default $V_n \sim U_n$, one can introduce the correction X_n so that $V_n = U_n + X_n$ and the recursion equation becomes

$$X_{n+1} - X_n = X_n - X_{n-1} + (g_c/2)X_n \tag{2}$$

for $n \geq 1$ and the boundary conditions (where we have set $E=1$ for simplicity)

$$\begin{aligned} &X_1 = (1+g_c/2)X_0 - 1 \ , \\ &X_n \to 0 \ \text{ as } n \to \infty \ . \end{aligned} \tag{3}$$

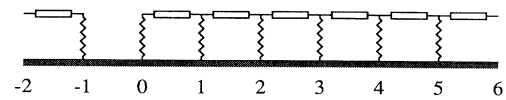

FIG. 3. One-dimensional version of the model shown in Fig. 2. The chain is the one-dimensional projection on the direction parallel to the field. The value of the conductances is here twice the value in the two-dimensional model.

To find the X_n one needs to solve the characteristic equation $\lambda^2 - (2+g_c/2)\lambda + 1 = 0$ whose roots $\lambda_\pm = (1+g_c/4) \pm \sqrt{g_c/2 + g_c^2/16}$ give the quantity X_n as $X_n = A\lambda_-^n + B\lambda_+^n$. Determining the constants by the boundary conditions one finds

$$X_n = \frac{(1+g_c/4 - \sqrt{g_c/2 + g_c^2/16})^n}{\sqrt{g_c/2 + g_c^2/16} + g_c/4} \ . \tag{4}$$

This expression shows that the correction X tends to zero exponentially with the distance. One can therefore write that $X_n \sim \exp(-n/\xi)$, where ξ is a characteristic length function of the solution of the characteristic equation, $\xi = -1/\ln(\lambda_-)$.

Figure 4 shows the evolution of ξ as function of g_c. Asymptotically, the following behaviors are obtained

$$\begin{aligned} &\xi \sim \frac{1}{\sqrt{g_c/2}} \quad \text{for } g_c \ll 1 \ , \\ &\xi \sim \frac{1}{\ln g_c/2} \quad \text{for } g_c \gg 1 \ . \end{aligned} \tag{5}$$

From the physical point of view this length represents the range of influence of a defect. At a distance larger than ξ the field is not affected by the absence of a fuse but only by the interaction with the substrate. At shorter distances instead the coupling with the substrate becomes less relevant and the field is mostly determined by the local configuration of fuses.

Let us emphasize that only screening effects are correctly described by the one-dimensional version of the model. In two dimensions, a crack which does not span the entire system will induce a large current concentration in the vicinity of its tips. This enhancement will also be localized in a zone of maximum size ξ.

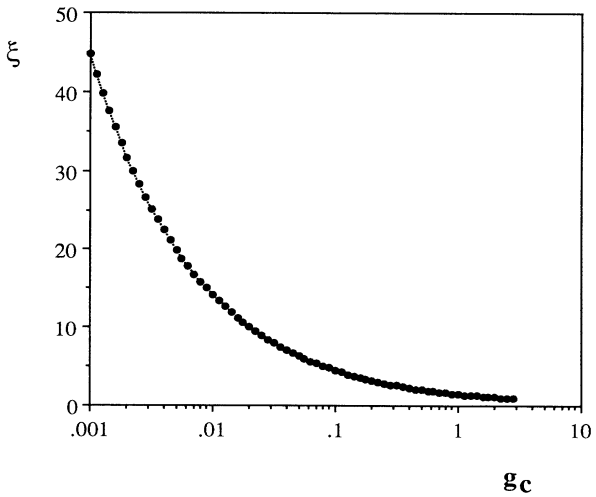

FIG. 4. The evolution of ξ as function of g_c as obtained in the one-dimensional model.

IV. BREAKING STRENGTH

The external field for which a bond breaks is given by the minimum over all bonds of the ratio of the local threshold over the local voltage drop. Thus two effects are competing: First, the enhancement of the current at the tip of a crack will favor a localized damage giving rise to a macroscopic crack, and second the minimization of the local threshold has the opposite tendency of spreading the damage evenly in the sample. This is the basis of the stabilizing effect of heterogeneities, which was mentioned in the Introduction. The two types of disorder considered will show two examples where these two effects have different weights, but we will first consider the case of the one-dimensional model.

A. One dimension

In one dimension, there is no enhancement of the current in the vicinity of a crack. In this case, the mapping from the two-dimensional model implies that the crack is spanning through the network, and thus no enhancement of the current is expected. Only the screening effect is reproduced. This screening has been studied in the previous section, and the current has been seen to be affected only in a region of size ξ around a crack. For a one-dimensional chain of length L, the weakest bonds will fail first. Let $P(j_c)$ be the cumulative distribution of breaking strength, and Φ the inverse function $P(\Phi(x))=x$. The weakest element in the chain has a threshold of the order of $\Phi(1/L)$. The nth weakest has a mean threshold of $\Phi(n/L)$. Suppose we pick the n weakest bonds in the chain. Those bonds are spatially uncorrelated and thus the distribution of distance between two consecutive bonds will be exponential. The average separation between two such bonds will be L/n. As long as this distance will be greater than ξ, we can neglect the decrease in current due to the vicinity of a crack. The macroscopic breaking voltage for the nth bond to break will thus be

$$V_c(n)\approx\Phi(n/L) \quad \text{for } n \ll L/\xi \ . \tag{6}$$

When the typical separation between broken bonds becomes closer to ξ, one should take into account the screening effect. This will increase V_c compared to the latter expression, which can be seen as a lower bound. Therefore, the damage will always be controlled.

B. Weak disorder

Before discussing the results we show in Fig. 5 some configurations of cracks at the final stage of the simulation. The four samples are obtained for a value of the coupling constant g_c ranging from 0.01 to 1.0. The periodic boundary conditions are explicitly shown by drawing four networks side by side. One sees clearly that the cracks are oriented perpendicularly to the field. Moreover, for a weak disorder and a large coupling length ($g_c=0.01$) only one large crack crosses the system, whereas several small cracks start to appear with a well-defined minimum distance between them as the coupling length becomes smaller than the lattice size.

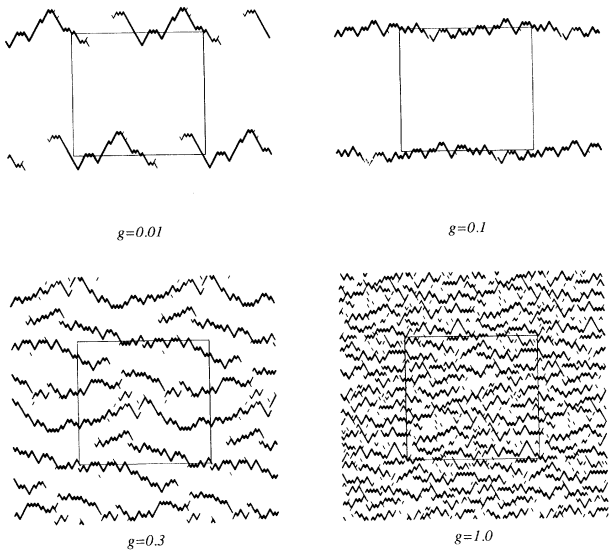

FIG. 5. Four configurations of cracks at the final stage of the simulation using our stopping criterion. The four samples are obtained for a system size $L=40$ and a value of the coupling constant g_c ranging from 0.01 to 1.0. The periodic boundary conditions are explicitly shown by drawing four networks side by side. All examples are obtained with a weak disorder. The thickness of the broken bonds is proportional to the local opening of the crack.

Since at each rupture step the value of the external potential is tuned so that only one fuse breaks at its threshold, it is easy to monitor the value of the external potential as function of the number of broken bonds n. Figure 6(a) shows the data for $g_c=0.01$. For small g_c we observe that the breaking voltage rapidly decreases as one crack is initiated. That means that a macroscopic crack appears abruptly in the system, and its propagation is self-sustained if the electric field is kept constant. As g_c increases this effect is less important, however, in the first stage of the process the breaking voltage still steadily decreases. For instance, for $g_c=1$ and a system size $L=20$ about 40 bonds have to break before reaching the same value of the potential as for the first broken bond. We have also carried out a few simulations letting the system evolve after one major crack has been created. In this case, after a first decrease, the breaking voltage appears to increase at the latter stage. This increase is attributed to the overall screening effect, which will progressively reduce the total current in the fuse network as more and more cracks are present, and the weaker effect of the enhancement of the current at the crack tips.

The case $g_c=0.3$ is particularly interesting since $1<\xi<L$ with easily accessible system sizes. Figure 5 shows that several parallel cracks are created before one of them reaches the size of the system. The breaking voltage of a single configuration presents strong fluctuations and reveals a sequence of strong peaks whose upper

envelope slowly increases. The breaking process is controlled over a long time range (as expected from the one-dimensional model). The voltage decrease due to fluctuations indicates that the rupture evolves by bursts, with several bonds breaking at the same time.

C. Strong disorder

The geometry of the crack configuration at the final stage of rupture becomes definitely richer in the presence of strong disorder in the breaking thresholds (Fig. 7). Also for a large coupling length cracks of all sizes are now present with a large crack spanning the system. As the coupling length becomes smaller the cracks evolve toward a denser configuration at the point where our stopping criterion is encountered (one spanning crack).

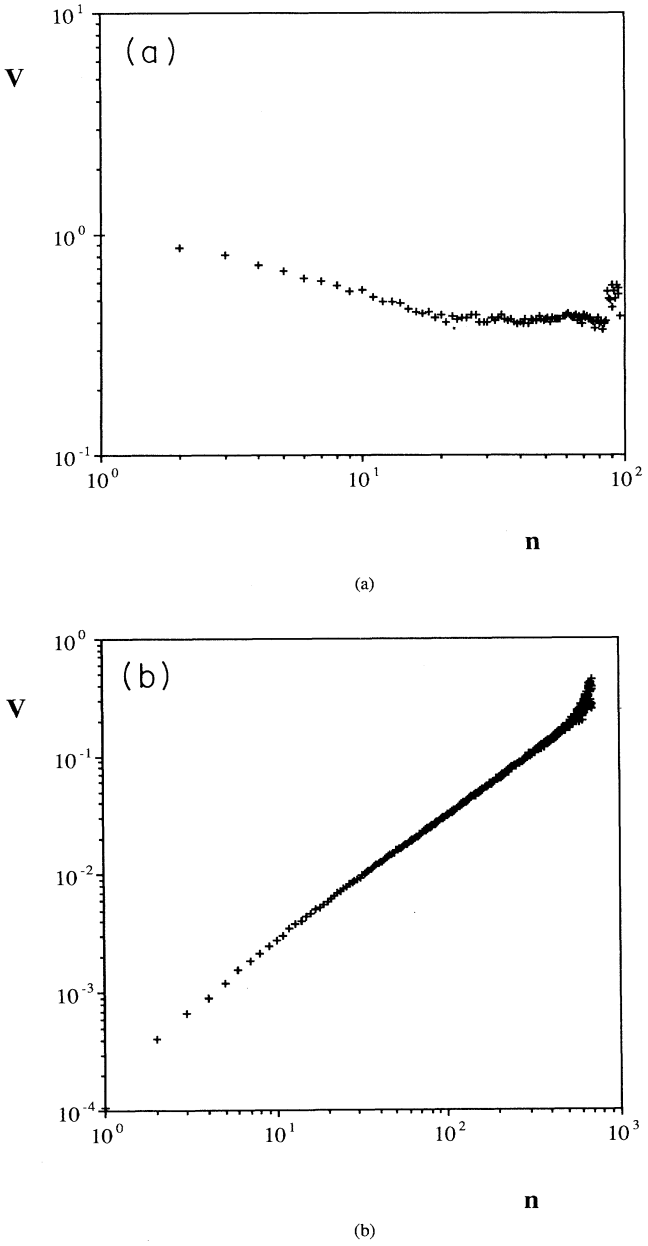

FIG. 6. External breaking voltage V as function of the number of broken bonds n for 50 configurations of system size $L=40$. The coupling parameter is $g_c=0.01$ for (a) weak and (b) strong disorder.

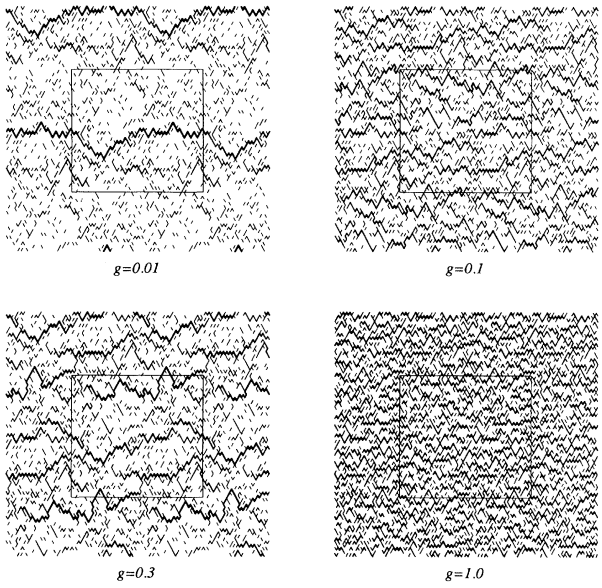

FIG. 7. Four configurations of cracks at the final stage of the simulation as in Fig. 5 for a strong disorder.

The breaking potential has in this case a very different behavior. V is here an increasing function of n [Fig. 6(b)], the process is then stable and the potential must be raised each time a bond has to break. The slope of the straight lines is approximately 1.0 for the three values of g_c analyzed, suggesting that the voltage drop on each bond is almost constant and that the process is controlled by the breaking thresholds. In fact, the breaking potential is the minimum over all the present fuses of the ratio j_c/j, where j is the current through the bond for a unit electric field and j_c its breaking threshold. If j is practically constant then the breaking potential is equivalent to the cumulated distribution of thresholds, that is $V(n)\approx n/L^2$.

The coupling length has a very weak influence in this case and mainly at the last stage of the process. One can observe in fact that for small values of g_c the potential tends to increase faster at the end of process. At this stage the local currents are reduced in the vicinity of a crack causing an increase in the breaking potential. The larger the value of the coupling length the sooner this effect comes into play. For instance, for small ξ (e.g., $g_c=1$) it does not appear.

V. CRACK OPENING

A. One dimension

A quantity of great interest to the engineers is the distribution of local opening of a crack in a given

TABLE I. Maximum crack opening for different values of the coupling parameter g_c. The table reports the values obtained for the one-dimensional model with one crack in an infinite system, and for the numerical simulations with weak and strong disorder in the thresholds.

	Maximum crack opening		
g_c	$1-d$	Weak disorder	Strong disorder
0.01	27.30	17.0	15.0
0.1	8.0	7.0	6.0
0.3	4.26	4.0	4.0
1.0	2.0	1.6	2.0

configuration. Within the framework of the one-dimensional model introduced in Sec. III, it is possible to calculate the opening of a single crack in an infinite system. The opening is defined in our model as the difference of potential at the two ends of a broken bond, minus the voltage drop imposed by the substrate. Following the notation introduced before this opening w can be expressed as

$$w=2X_0=\frac{2}{g_c/4+\sqrt{g_c/2+g_c^2/16}}\ , \tag{7}$$

which gives qualitative information on the evolution of

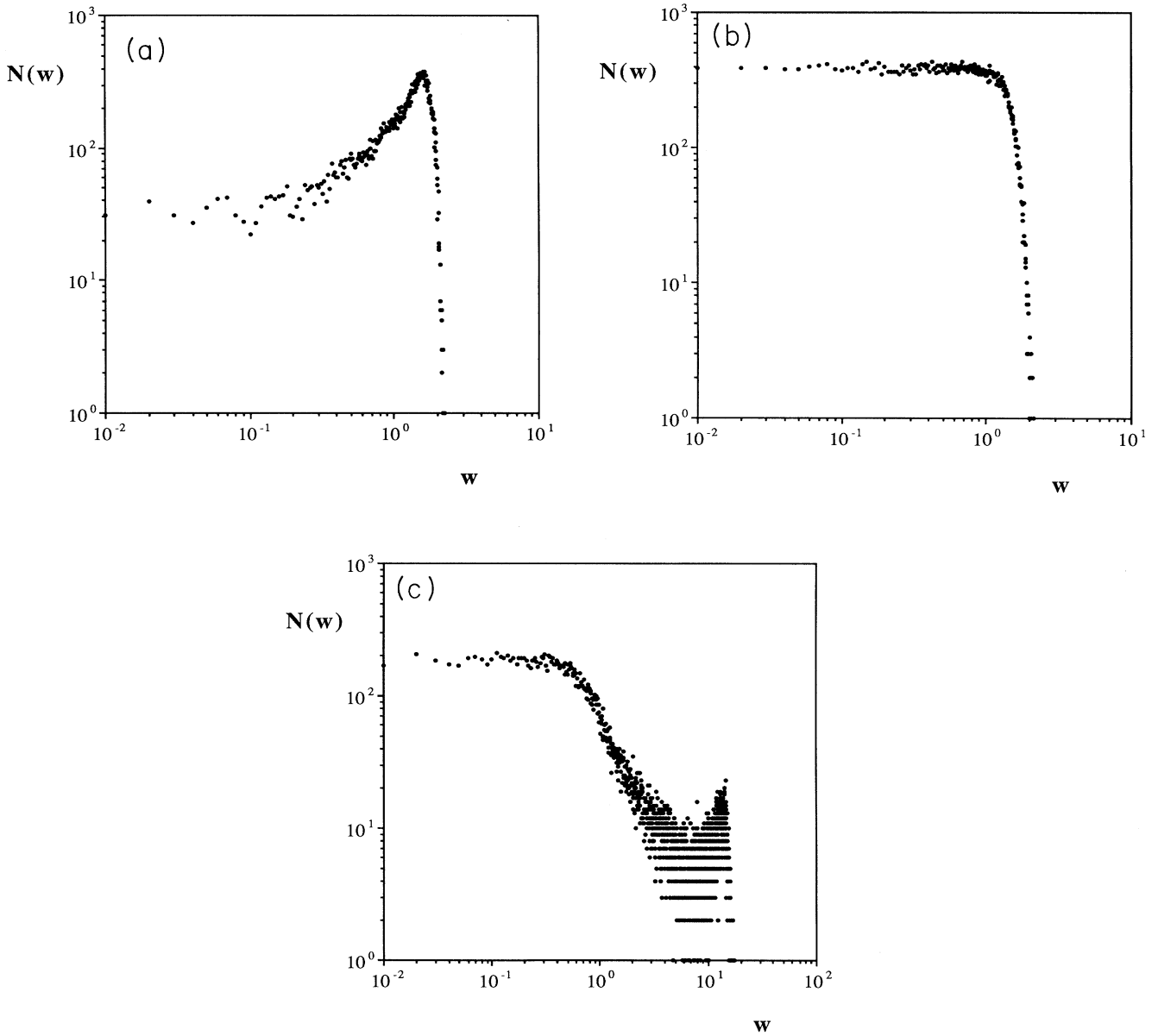

FIG. 8. Distribution of crack opening $N(w)$ at the last stage of the rupture process for 200 configurations of system size $L=20$: (a) for weak disorder and $g_c=1.0$; for strong disorder and $g_c=1.0$ (b) and 0.01 (c).

the crack opening with g_c (Table I).

This simple calculation can easily be generalized by introducing two cracks in the system separated by a distance δ in order to evaluate the crack opening as a function of the relative distance. At small distance w is proportional to δ and independent of ξ (and thus g_c). At a distance larger than a few ξ the opening becomes independent of δ and reaches a value 2ξ that corresponds to the solution (7) found for an infinite system.

B. Weak disorder

We analyze numerically the distribution of crack opening at the last stage of the rupture process, according to our stopping criterion. The data show a very pronounced peak [Fig. 8(a)] at a value of the maximum opening very close to the predictions of the one-dimensional model (Table I). This simple model gives then a good estimate in the case of weak disorder where the geometry of the cracks is well described by a set of periodically spaced linear cracks.

We have also analyzed the scaling properties of the moments of the distribution as function of L. The data show that they follow constant gap scaling for both values analyzed $g_c=0.01$ and 1.0. This result indicates that there is a characteristic opening controlling the critical behavior of all the moments of the distribution.

C. Strong disorder

The behavior of the distribution of crack openings is rather different in this case. Figures 8(b) and 8(c) show a distribution almost uniform for small opening values. As the coupling constant g_c decreases a peak develops at large w and progressively separates from the bulk of the distribution. This peak corresponds to the macroscopic crack where the wide opening concentrates, whereas the isolated microcracks are less open. To support this picture, one can notice that the value of the maximum opening is in good agreement with the result from the one-dimensional model (Table I). Furthermore, the height of the peak, which gives the number of broken bonds belonging to the macroscopic crack, is as expected inversely proportional to the coupling length ξ and therefore proportional to the maximum crack opening.

The study of the scaling behavior of the moments of the distribution as function of L shows that constant gap scaling is followed for small ξ (i.e., $g_c=1.0$). We find, however, that there is some evidence for a more complex scaling at large values of the coupling length ($g_c=0.01$). We analyzed then the moments as function of ξ for a system size $L=40$ (Fig. 9) over a range of coupling lengths smaller than L. The data indeed exhibit multifractal behavior[15] over the range of length considered, that is the different q moments, appropriately rescaled, follow straight lines whose scope is not constant (constant gap scaling) but depends on q.

Finally, we performed the same analysis for the case of a zero interaction with the substrate ($g_c=0.0$). In this case our model reduces to a model for fracture of an heterogeneous system studied in the literature. In a previous study,[13] multifractal behavior was detected for the distribution of local currents at the last stage of rupture. We found that also the distribution of crack openings has a multifractal behavior for this model.

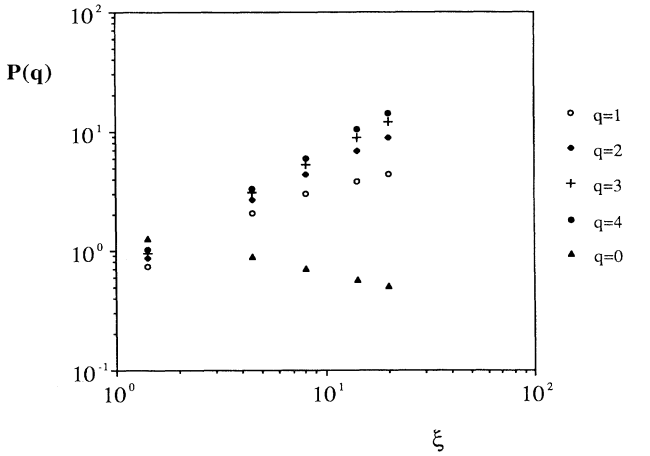

FIG. 9. Renormalized moments of the opening distribution, $P(q)=[M(q)/M(0)]^{1/q}$, for $q=1,\ldots,4$ and the average zero moment $\langle M(0)\rangle$ as a function of ξ for 50 configurations of a system size $L=40$.

VI. GEOMETRICAL PROPERTIES

A. Weak disorder

Each time a new bond is broken we monitor the number of distinct cracks (e.g., connected clusters in the dual of the fuse network) present in the system N_c. For small values of the coupling parameter basically one or a few cracks develop in the system (Fig. 5). As can be seen in Fig. 10, the number of cracks remains indeed constant and close to one for most of the evolution and independently of the system size. For $g_c=0.1$, for instance, $N_c\approx 1.5$, which indicates that two cracks are initiated but only one propagates to span through the system. Beyond this stage, that corresponds to our stopping criterion, another crack will eventually be initiated, propagate, and the process then will go on.

For small values of ξ ($g_c=1$) many cracks are instead present in the system. Their number increases with n, indicating that many microcracks are initially created. The height of the maximum depends on the system size (it is for instance equal to 27 in a system $L=20$) but the density of cracks at the maximum is constant, that is the number of cracks is proportional to L^2. Beyond this point N_c starts to decrease suggesting that small cracks interact among them and coalesce contributing to the formation of a spanning macroscopic crack. The intermediate case, $g_c=0.3$, shows a similar behavior but with a lower density of cracks at the maximum due to the larger range of the interactions.

At the final stage of the process we study the geometrical properties of the configuration of cracks obtained. We start by analyzing the distribution of distances between

cracks. This consists in calculating the distance separating two cracks along the direction parallel to the applied electric field. The distribution of such distances shows a very different behavior for g_c larger and smaller than 0.3 (Fig. 11). For a strong coupling the distribution is an exponential $N(\delta) \sim \exp -(\delta/d)$, where d is a typical separation between two cracks. This characteristic distance is close to 1.5 for $g_c = 1$ and $L = 40$ and slightly decreases as the system size increases. For a small coupling, the distribution of distances is instead rather uniform over the whole range of δ.

During the breaking process we also measure the number of broken bonds, i.e., the mass M, of the major crack and its extension in the directions parallel (Y) and perpendicular (X) to the field. In this way, we can analyze the fractal properties of the largest crack during its evolution. The fractal dimension of the crack—such that $M \propto X^{d_f}$—is, as expected, close to one,[12,13] $d_f \approx 1.15$ for $g_c = 1$ and $d_f \approx 1.05$ for $g_c = 0.01$.

Furthermore, we analyze the roughness of the macroscopic crack, $Y(X)$ (Fig. 12). We find that the width of the crack is definitely smaller than its length. We investigate the self-affinity of cracks by searching for an eventual power-law relation $Y \propto X^{\zeta}$. The evolution of the exponent ζ gives interesting insights on the range of correlations in the system. In fact, if linear cracks were randomly connected, the expected value of the exponent would be 0.5 as for a biased random walk. If, on the con-

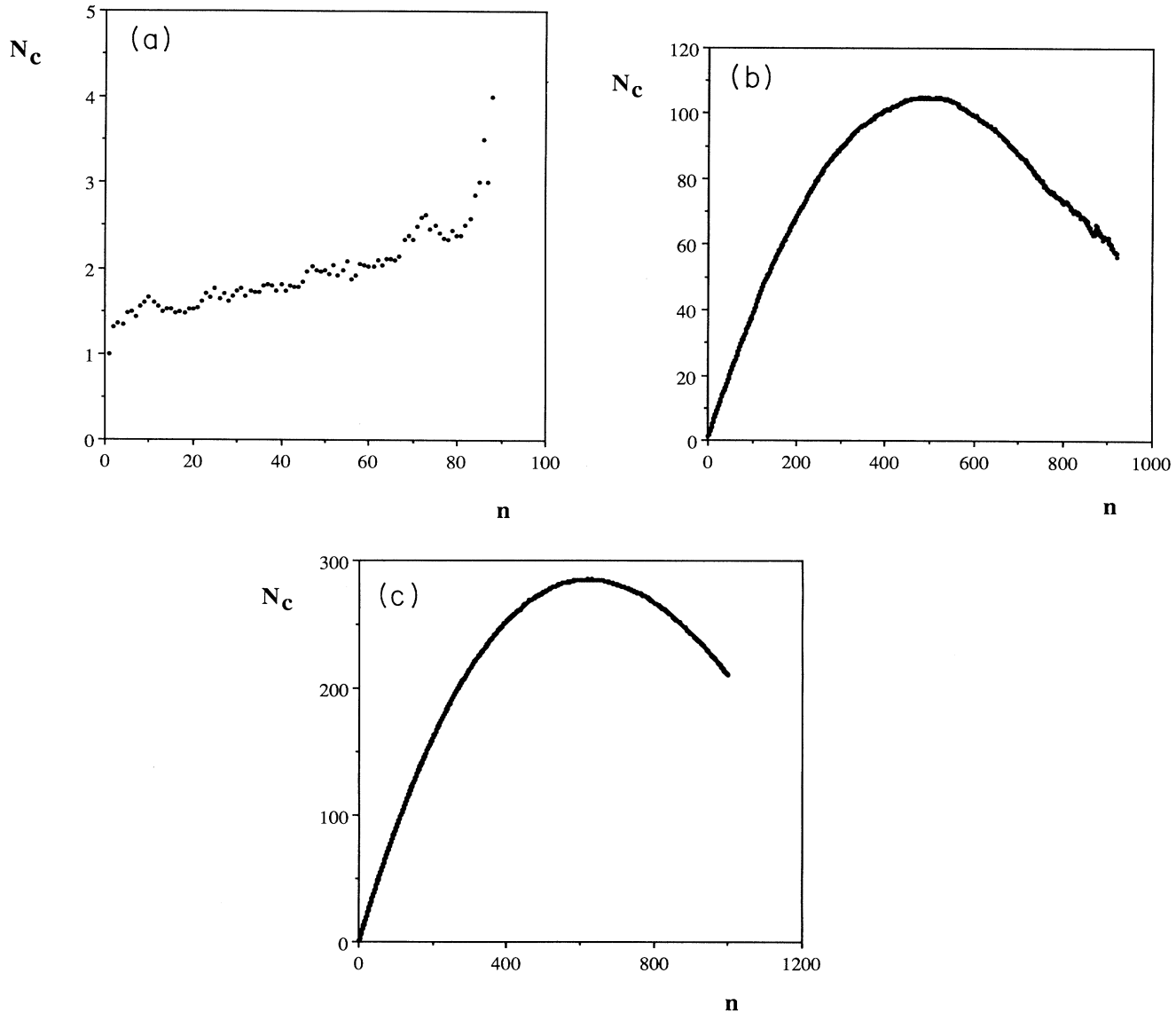

FIG. 10. Number of cracks (clusters) N_c as a function of the number of broken bonds n for 50 configurations of system size $L = 40$: for weak disorder and $g_c = 0.1$ (a) and 1.0 (b); for strong disorder and $g_c = 1.0$ (c).

trary, the coupling with the substrate did not play any significant role, one would expect to find the property of self-affinity already detected in a fuse network model with a usual loading[16] with an exponent $\zeta \approx 0.77$ in two dimensions. We find that for a small value of the coupling length the data follow the first behavior ($\zeta \approx 0.5$). As ξ increases, the exponent ζ also increases and reaches the value $\zeta \approx 0.7$ for $g_c = 0.01$.

From the ensemble of results, it appears that in the case of weak disorder a characteristic length scale exists separating two distinct regimes. At a scale larger than this length (or for small g_c) the breaking process is similar to the one observed for systems, where the external load is applied in the usual way. More precisely, the case for the electric analog is a two-dimensional fuse network where a difference of potential is applied between opposed boundaries. The coupling with the substrate does not play any significant role and the macroscopic crack is mainly linear and self-affine. At a smaller scale (or for large g_c) the microcracks do not interact among themselves and the macroscopic crack pattern is formed by the random superposition of independent contributions.

B. Strong disorder

The number of cracks (clusters) present in the system as function of the number of broken bonds (Fig. 10) in

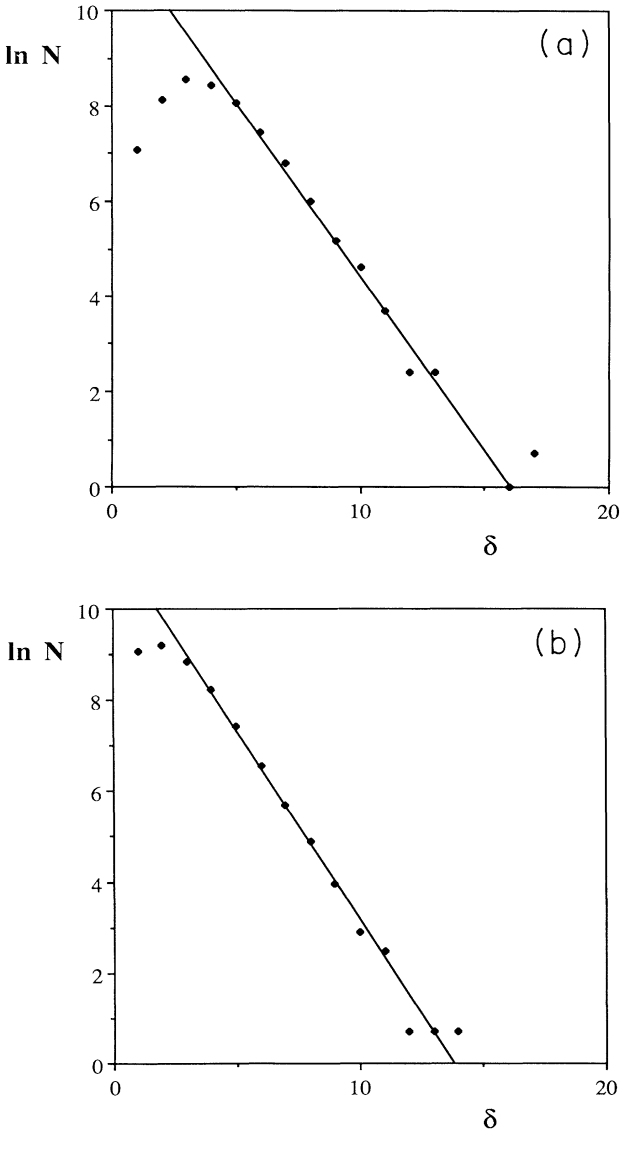

FIG. 11. Distribution of distance between cracks $N(\delta)$ at the last stage of the rupture process for 50 configurations of system size $L = 40$ with $g_c = 1.0$ for (a) weak and (b) strong disorder. The inverse value of the slopes are given in Table II.

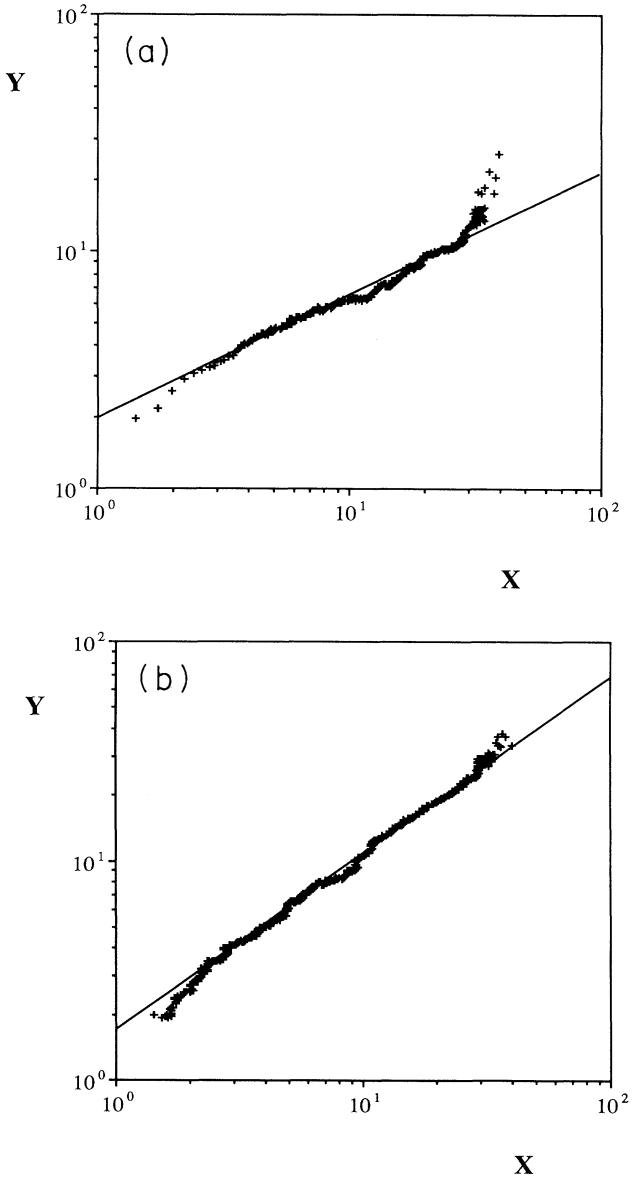

FIG. 12. Roughness of the largest crack, $Y(X)$, as a function of its extension for $L = 40$ and $g_c = 1.0$. The straight lines show an exponent $\zeta \approx 0.5$ for a weak disorder (a) and $\zeta \approx 0.9$ for a strong disorder (b).

this case has a behavior similar to the one found previously for small coupling lengths for all g_c. $N_c(n)$ shows an initial increasing phase, where many microcracks are created, then reaches a maximum beyond which cracks start to coalesce and $N_c(n)$ rapidly decreases. The maximum number of cracks does not appear to depend on g_c but it is proportional to the number of fuses in the system L^2. The value of n at which the function reaches its maximum n^* is also quite independent of g_c and proportional to L^2 as well. The expected behavior is given in fact by the superposition of $(L/\xi)^2$ subsystems of size ξ, where the coupling with the substrate becomes unimportant and it was found $n^* \propto \xi^{1.8}$.[13] Therefore $n^* \propto (L/\xi)^2 \xi^{1.8} \propto L^2 g_c^{0.1}$. Our data are in agreement with a slow increase of n^* with g_c.

The distribution of distances between cracks here exhibits an exponential behavior for all values of g_c (Fig. 11) for large separation δ, and a smaller density for $\delta < \xi$. The characteristic separation d varies as expected with g_c (Table II), that is it increases as the coupling length increases, and depends on the disorder and the system size. The stopping criterion for the process, since the quantities are measured on the final configuration of cracks, might also influence the value of d. These estimates of d take into account the repulsion effect between parallel cracks that can be seen in Fig. 7. However, the structure at large scale that appears for small g_c, does not come out from this analysis, since the evaluation of d is not sensitive to the size of the cracks.

The evolution of the mass of the largest crack as function of its size perpendicularly to the field gives the fractal dimension, estimated to be approximately 1.3 for $g_c = 0.01$ and 0.1. However, in the limit $g_c = 0$ our model reduces to a well-known fracture model, in this case a fractal dimension approaching 1 as the system size increases was observed, and thus the above-mentioned apparent fractal dimension may be due to strong size effects. The data for $g_c = 1$ are slightly curved with an average slope of 1.5.

The width of the crack is always smaller than its size, since the cracks are aligned perpendicularly to the field. The straight lines (Fig. 12) scale with an exponent $\zeta \approx 0.8$ for $g_c = 0.01$ and 0.1, and $\zeta \approx 0.9$ for $g_c = 1$. The value of ζ for small g_c is in good agreement with the value found for usual fracture models,[16] where the property of self-affinity has been detected with an exponent $\zeta \approx 0.77$.

The analysis of the data indicates that the breaking process is driven by the disorder in the thresholds and that the electric field is quite irrelevant at least at the first stage of the process. It is, therefore, interesting to compare the fractal dimension obtained in this case with the one obtained from a model where the disorder is the only breaking criterion (*percolation limit*).[17] The model is a random network of fuses, where the element with the lowest threshold is broken each time. The problem becomes purely geometrical and it has been widely studied in the past.

TABLE II. Characteristic separation from the numerical simulations with strong disorder for different values of g_c. The values reported are the inverse slope of the semilog plot of the distribution of distance cracks for the system sizes $L = 20$ and 40.

	Characteristic crack separation	
g_c	$L = 20$	$L = 40$
0.01	3.4	3.5
0.1	1.8	1.6
1.0	1.4	1.2

For this model two behaviors have been detected: If the fraction of broken bonds is close to zero the clusters obtained are known as *animals*[18] and have a fractal dimension of the order of 1.53 in two dimensions. If instead one is close to the percolation threshold, the fractal dimension of the percolation cluster, 1.89, is recovered. We have performed a numerical simulation in this case of infinite disorder with our precise geometry and range of sizes. We found that the fractal dimension varies continuously from the animal limit at the first stage of rupture to the percolation value, with an average slope of 1.55. On the other hand, since there is no electric field in this model, the cracks are isotropic and the width is proportional to the size ($\zeta = 1$). We find then that for the case of strong disorder and for small coupling length, that is for cracks weakly interacting with each other, the results are in agreement with the case of infinite disorder: The fractal dimension is about equal to 1.5 and the cracks are isotropic ($\zeta \approx 1$).

We note that a conclusion similar to the one obtained for a small disorder is obtained: At a small scale (smaller than ξ), the system behaves as expected in the absence of coupling to a substrate. The cracks appear to be self-affine with a similar exponent as the one already obtained in previous works. Above the coupling length, cracks do not interact and the system can faithfully be described as the superposition of independent subnetworks. In particular a percolationlike behavior can be identified in the limit of a strong disorder and small coupling length. For intermediate cases, a crossover is expected, however, the small system sizes considered did not allow us to see clearly the crossover between the two identified behaviors but rather apparent power laws with exponents whose value continuously varies from one case to the other.

VII. CONCLUSIONS

The model we have studied has revealed the role and importance of an intermediate length scale, which has been traced back to the coupling between the two layers (the fuse network and the substrate). This length scale separates a small scale regime where the loading does not seem to play any fundamental role, and a large scale regime where cracks do not interact with each others. We have identified in different properties the effect of this intrinsic length scale. This study may stimulate the precise measurement of this length scale in experimental tests as the one described in the Introduction in order to determine the scale at which the delocalization of the starting field will be effective.

The comparison with fractures induced by drying in materials such as clay, is more difficult. In our model, we

have lost the isotropic nature of the shrinkage. However, a few qualitative comparisons can be made. The fact that the maximum crack opening increases as the thickness (and thus the coupling length in our model) increases is well known. Moreover, the characteristic separation between cracks for strong disorder increases in our model with the coupling length. It is experimentally observed that plaquettes of larger thickness fracture, in fact, with fewer but wider cracks. Furthermore, for small thicknesses the characteristic separation decreases as the system size increases, in agreement with the experimental observation that larger samples exhibit a denser crack configuration. Finally, the fractal dimension obtained in the case of strong disorder is in fair accordance with the experimental values, albeit a quantitative agreement was not expected.

ACKNOWLEDGMENTS

We thank J. P. Hulin for useful discussions on this subject. We acknowledge the support of the Greco Géomatériaux, and the Groupement de Recherche Physique de Milieux Hétérogènes Complexes. Laboratoire de Physique et Mécanique des Milieux Hétérogènes is Unité de Recherche Associée au CNRS No. 857.

[1] *Statistical Models for the Fracture of Disordered Media,* edited by H. J. Herrmann and S. Roux (North-Holland, Amsterdam, 1990).

[2] *Disorder and Fracture,* edited by J. C. Charmet, S. Roux, and E. Guyon (Plenum, New York, 1990).

[3] J. Mazars and Z. P. Bažant, *Cracking and Damage* (Elsevier, Amsterdam, 1989).

[4] J. Mazars, S. Ramtani, and Y. Berthaud, in *Cracking Damage,* Ref. 3.

[5] D. Breysse and D. Fokwa, in *Fracture Processes in Concrete Rock and Ceramic,* edited by S. G. van Mier, J. G. Rots, and A. Baker (E. & F.N. Spon, London, 1991), p. 149.

[6] H. Colina (unpublished).

[7] P. Meakin, Thin Solid Films **151**, 165 (1987).

[8] W. A. Curtin, J. Am. Ceram. Soc. **74**, 2837 (1991).

[9] F. Hild (unpublished).

[10] A. Hansen, S. Roux, and H. J. Herrmann, J. Phys. (Paris) **50**, 733 (1989).

[11] H. J. Herrmann, A. Hansen, and S. Roux, Phys. Rev. B **39**, 637 (1989).

[12] L. de Arcangelis, A. Hansen, H. J. Herrmann, and S. Roux, Phys. Rev. B **40**, 877 (1989).

[13] L. de Arcangelis and H. J. Herrmann, Phys. Rev. B **39**, 2678 (1989).

[14] K. Khang, G. G. Batrouni, S. Redner, L. de Arcangelis, and H. J. Herrmann, Phys. Rev. B **37**, 7625 (1988).

[15] G. Paladin and A. Vulpiani, Phys. Rep. **156**, 147 (1987).

[16] A. Hansen, E. L. Hinrichsen, and S. Roux, Phys. Rev. Lett. **66**, 2476 (1991).

[17] S. Roux, A. Hansen, H. J. Herrmann, and E. Guyon, J. Stat. Phys. **52**, 237 (1988).

[18] D. Stauffer, *Introduction to Percolation Theory* (Taylor and Francis, London, 1985).

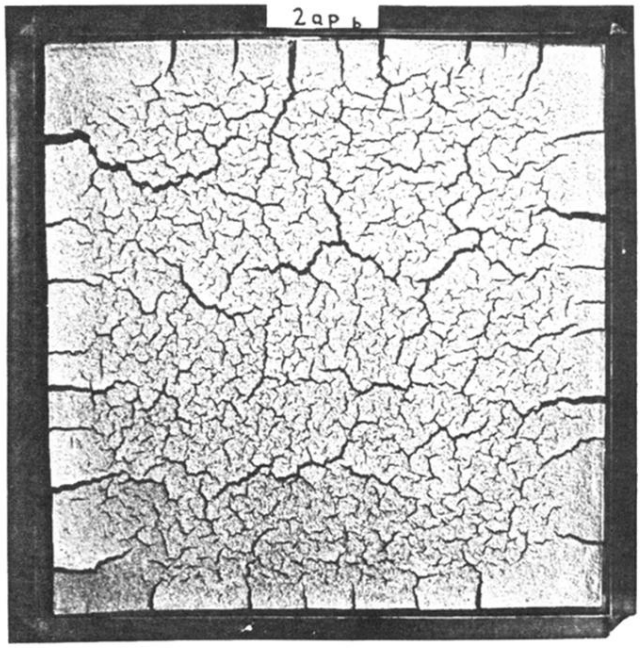

FIG. 1. Fracture pattern obtained on a thin layer of clay (20 cm × 20 cm × 2 mm). The cracks were created as a result of the shrinking of the clay after drying for about 7 h.